RECEIVED
MAR 0 4 1999

RF/ MICROWAVE NON-DESTRUCTIVE MEASUREMENTS OF ELECTRICAL PROPERTIES OF SEMICONDUCTOR WAFERS FOR THERMOPHOTOVOLTAIC APPLICATIONS

G. Charache, S. Saroop, et. al.

May 1997

DISTRIBUTION OF THIS DOCUMENT IS UNLIMITED

MASTER

DISCLAIMER

DISCLAIMER

Portions of this document may be illegible in electronic image products. Images are produced from the best available original document.

RF/Microwave Non-Destructive Measurements of Electrical Properties of Semiconductor Wafers for Thermophotovoltaic Applications

S. Saroop[†], J. M. Borrego[†], R. J. Gutmann[†], H. Ehsani[†], I. Bhat[†],
S. Dakshina Murthy[†], A. Ostrogorski[†], P. Dutta[†], M. Freeman[*], G. Charache[*]

[†] Center for Integrated Electronics and Electronics Manufacturing,
Department of Electrical, Computer, and Systems Engineering
Rensselaer Polytechnic Institute, Troy, New York 12180

[*] Lockheed Martin Inc., Schenectady, New York 12301

Abstract — A radio-frequency/microwave measurement system has been designed for non-contacting determination of sheet resistance and excess carrier lifetime of low-bandgap materials and junctions, specifically GaSb-based alloys for thermophotovoltaic (TPV) applications. The design incorporates RF circuitry in the 100-500 MHz frequency range and utilizes a Q-switched YAG laser at 1.32 microns to photo-generate electron-hole pairs and conductivity modulate the material and/or junction under test. Supplementary measurements with a GaAs pulsed diode laser at 904 nm provides a faster transient response with near-surface photogeneration. Initial measurements on GaSb substrates, Zn-diffused materials and epitaxially grown layers are presented and discussed.

INTRODUCTION

Conductivity, mobility and excess carrier lifetime are the three basic material parameters which influence the efficiency of thermophotovoltaic (TPV) cells. Conductivity and mobility are determined traditionally from Hall effect measurements, and excess carrier lifetime by several steady state and transient measurements on specially fabricated test structures. These techniques require the formation of ohmic contacts or the fabrication of a complete device and are destructive by nature.

A waveguide microwave reflection technique operating at Ka-band (36 GHz) was previously developed in our laboratory to measure the resistivity of wafers in the range of 10 Ω-cm to 1000 Ω-cm and, with the use of GaAs and AlGaAs pulsed lasers, to measure excess carrier lifetimes longer than 10 nanoseconds[1-5]. In this work the use of the photoconductivity decay to measure recombination lifetime in silicon wafers[1] and to characterize the defect free zone in precipitated CMOS wafers was demonstrated[2]. The techniques were also applied to GaAs using both above-bandgap and below-bandgap excitation to characterize both starting semi-insulating wafers[3] and ion-implanted channels for field-effect transistor (FET)-based integrated circuits[4]. The technique has even been successfully applied to semi-insulating InP wafers where both lasers were above-bandgap, but the effective absorption depth was significantly different[5]. With key information in the compound semiconductors available from the pulse amplitude response, mapping of the wafer surface can be used to plot defect structural information [6,7].

1

In this paper, the modifications performed in the microwave reflection system to allow measurement of semiconductor wafers with resistivity as low as 0.01 Ω-cm and excess carrier lifetimes larger than 100 ns (present limitation 0.7 μs) are presented. Initially, the measurement concept is described, followed by a first-order calculation of laser power required for conductivity modulation. Then the measurement technique implementation is presented, followed by the GaSb-based semiconductor materials and junctions evaluated. While a full understanding of these results has not been realized to date, the measurement system is clearly able to discriminate similar materials demonstrating that such an approach is useful for characterization and screening of TPV materials and junctions.

RF/MICROWAVE REFLECTION CONCEPT
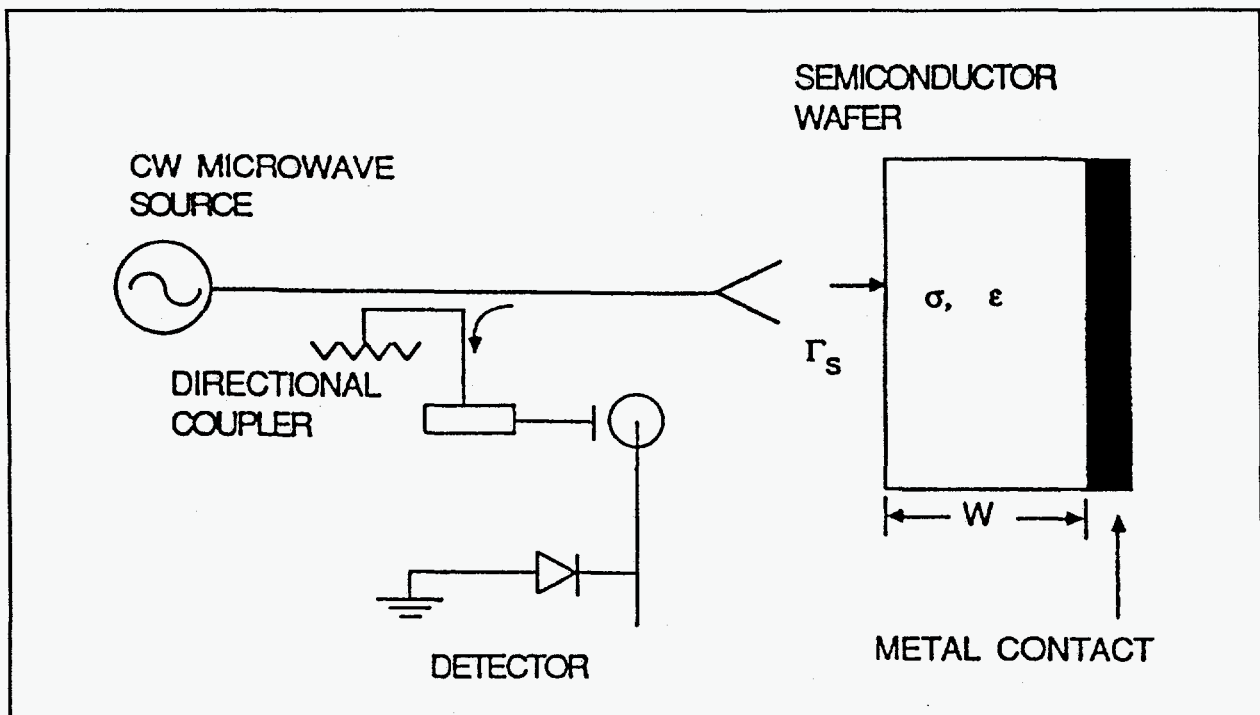
Figure 1. Microwave Reflectance System

A schematic diagram of a microwave reflection system is shown in Figure 1. A microwave source provides continuous microwave power which is incident on the sample, and the reflected power is measured using a directional coupler and a microwave detector. The reflected power depends upon the conductivity, dielectric constant and thickness of the sample and the frequency of the continuous-wave (CW) microwave source. Thus, the conductivity of the sample can be determined from the measurement of the reflection coefficient. In addition, the excess carrier lifetime can be measured by recording the decay of excess carriers by monitoring the change in the reflected power after the generation of hole-electron pairs by a pulsed monochromatic light source.

In the measuring system shown in Figure 1, the voltage reflection coefficient, Γ_s, of the

2

wafer is given by:

$$\Gamma_S = \frac{Z_S - Z_O}{Z_S + Z_O} \tag{1}$$

where Z_S is the wave impedance of the wafer at the top surface of the wafer and Z_0 is the wave impedance of the microwave incident upon the wafer. Assuming that the wave impedance of the wafer is purely resistive and given by R_S, the reflection coefficient is determined by the normalized sheet resistance of the wafer $R_{SN} = R_S / Z_0$. The normalized reflected power $|\Gamma_S|^2$ as a function of the normalized sheet resistance of the wafer is shown in Figure 2. The figure shows that measurement of wafer sheet resistances in the range of $0.1 Z_0 < R_S < 10 Z_0$ is possible. Assuming that the microwave incident upon the wafer has a wave impedance like in a waveguide, i.e., 500 Ω, the sheet resistances which can be measured in a waveguide system are in the range between 50 and 5000 $\Omega/\square$. If the wafers have a thickness of approximately 0.020 inches, the wafer resistivities which can be measured are in the range between 2.5 Ω-cm and 250 Ω-cm.
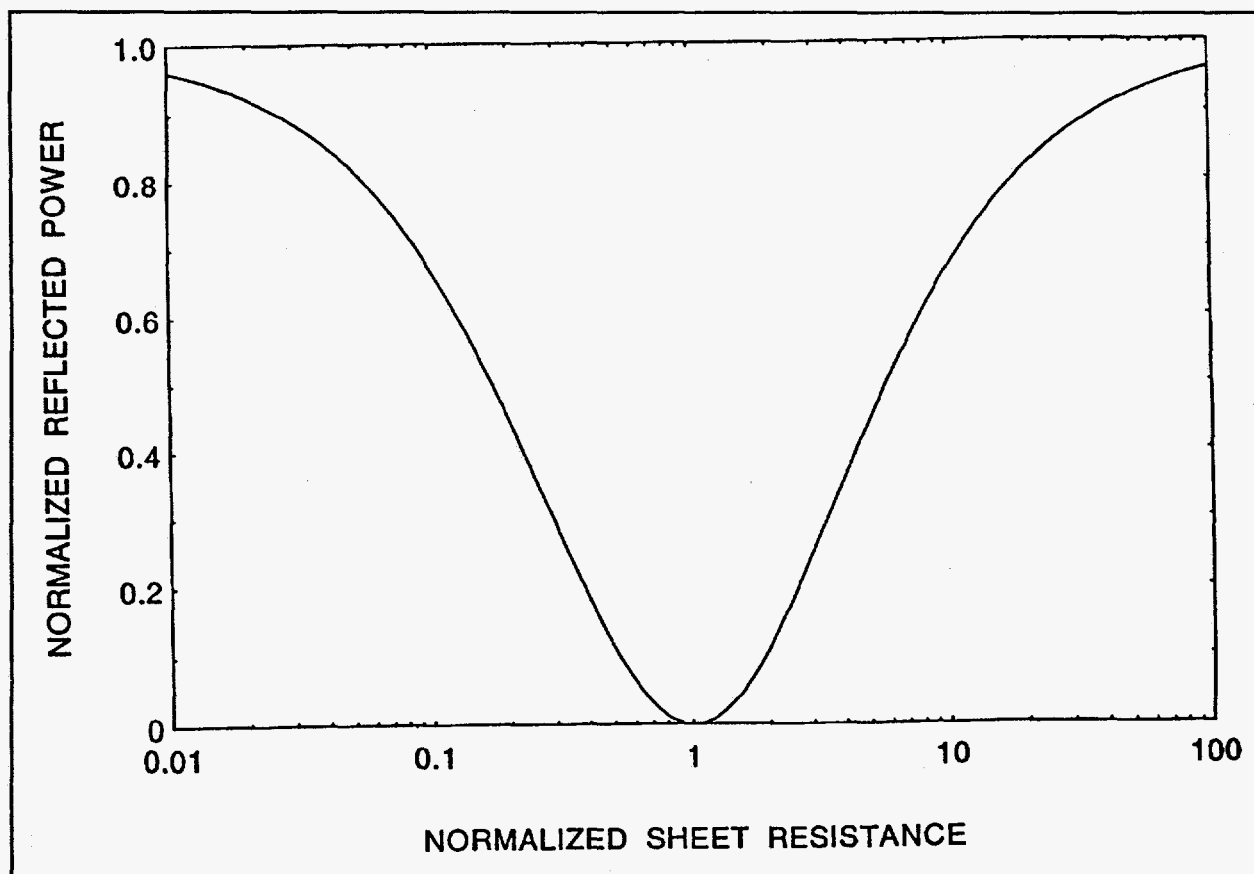

Figure 2. Normalized Reflected Power vs. Normalized Sheet Resistance

This first-order analysis gives the approximate range of wafer resistivity which can be measured with a waveguide resistivity probe. In order to measure lower resistivity wafers a measurement system with a lower characteristic impedance is required and/or a transformer is

3

needed which changes the sheet resistance of the wafer measured by the measurement system. Both approaches have been used in an RF measurement system which is more suitable for high-conductivity low-bandgap materials of interest for TPV applications.

In order to lower the range of resistivity which can be measured by a microwave reflection system, a coaxial measuring system with a wave impedance of 50 Ω and a transformer to couple the wafer being measured to the measurement system were utilized. While this 50 Ω coaxial system would allow one to measure wafers with resistivity in the range of 0.25 Ω-cm to 25 Ω-cm, this range is not low enough to measure semiconductor wafers for TPV cells. An impedance transformer is used to transform the sheet resistance of lower resistivity wafers to the appropriate range of the RF coaxial system. In order to be able to build impedance transformers without significant parasitics, the frequency of operation of the measurement system was lowered to be in the RF frequency range. However, the frequency has to be large enough to measure transient decays larger than 50 or 100 ns. As a compromise, the system was designed to operate in the frequency range of 100 to 500 MHz using instrumentation similar to that introduced by Yablonovitch[8].
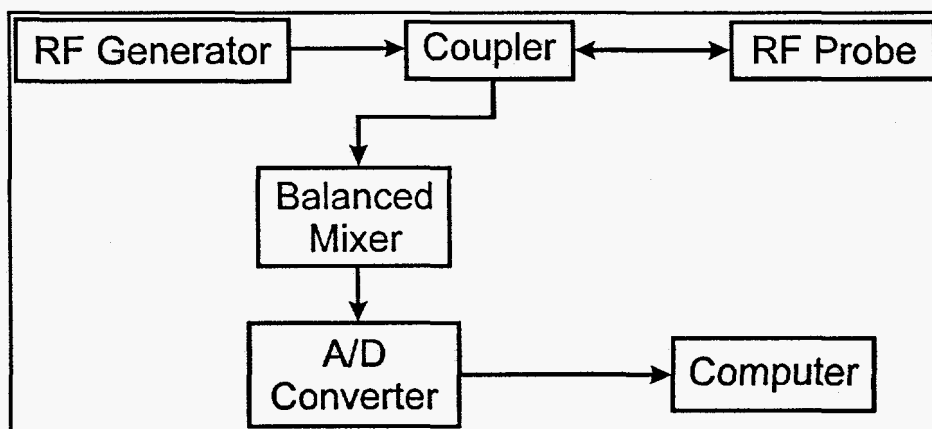

Figure 3. RF Resistivity Probe Schematic

Figure 3 is a schematic diagram of the RF resistivity probe measurement circuit, consisting of an RF generator with two outputs. The variable output provides the RF signal which is sent to the wafer through a directional coupler. The reflected signal is directed by the directional coupler to the signal input of a balanced mixer. The fixed output of the RF generator is sent to the local oscillator (LO) input of the balanced mixer. The intermediate frequency (IF) output of the balanced mixer is then digitized and then sent to an IBM PC.

The same setup can be used for measuring the lifetime of excess carriers. By the addition of a pulsed laser, the transient decay of the photoconductivity induced by a pulsed light source can be monitored with the digital oscilloscope. Figure 2 shows that a change in the sheet resistance, as caused by a light source, translates into a change in the power reflected for the microwave direct detection system of Figure 1. Note that if the normalized dark sheet resistance is exactly at the minimum of the curve (i.e. the normalized sheet resistance is equal to unity), the power reflected does not change with optical excitation. However, in the homodyne detection

4

system implemented here, the detected signal is proportional to Γ_S (rather than $|\Gamma_S|^2$), so that high sensitivity can be achieved around a DC operating point where $\Gamma_S=0$.

The effect of the frequency of operation of the RF resistivity probe upon the range of wafer resistivity which can be measured using the skin depth as a function of wafer resistivity and measurement frequency was analyzed. The resistivity probe measures sheet resistance, R_S, which is given by the ratio of the wafer resistivity, ρ, to either the skin depth, δ, or the wafer thickness, t, depending upon thickness. That is:

$$R_S = \frac{\rho}{\delta}, \qquad \delta < t$$
$$\quad = \frac{\rho}{t}, \qquad \delta > t \tag{2}$$

where the skin depth, δ, is given by the equation:

$$\delta = \sqrt{\frac{2\rho}{\omega\mu}} \tag{3}$$

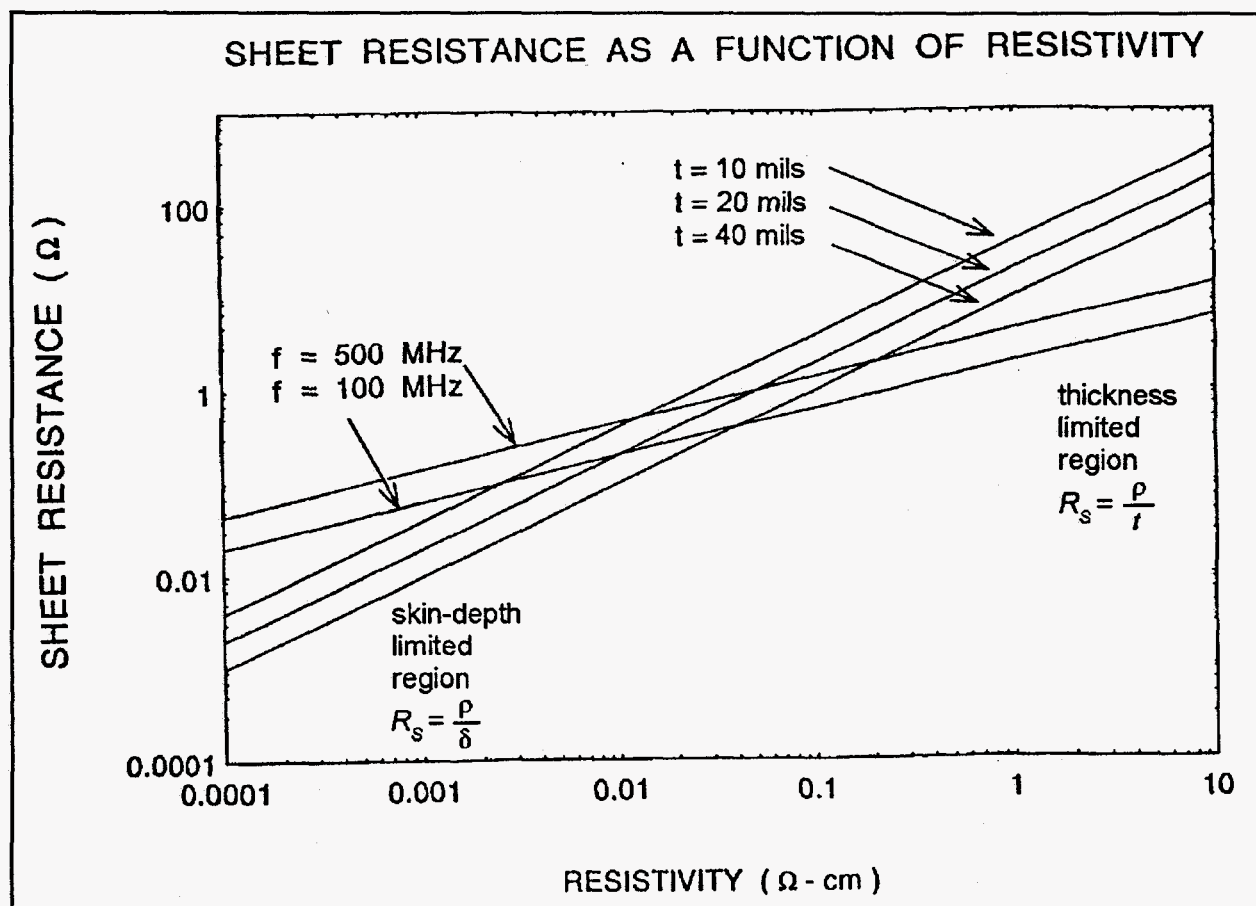## SHEET RESISTANCE AS A FUNCTION OF RESISTIVITY

Figure 4

5

Figure 4 shows a plot of Equation 2 for frequencies of 100 and 500 MHz and for wafer thicknesses of 10, 20 and 40 mils as a function of wafer resistivity. The figure shows that the resistivity probe should be able to measure sheet resistances between 0.1 and 10 Ω. However, in order to be able to measure wafers with resistivity between 0.001 and 0.1 Ω-cm, a coaxial system with characteristic impedance of 50 Ω and some type of transformer to couple the wafer to the measurement system are required.

An analysis of the impedance, Z, of a flat coil coupled to a semi-infinite slab of conductivity, ρ, resulted in the following expression for the terminal impedance of the coil:

$$Z_S = \frac{\rho}{\delta} N_T^2 A (1+j) \tag{4}$$

where N_T is the number of turns per unit length and A is the area of the coil. The above equation shows that a flat coil of an appropriate area and turns per unit length may be needed to measure the desired range of wafer resistivity.

In order to connect the flat coil or transformer to the coaxial measuring system shown in Figure 2, an appropriate microstrip circuit was designed. A coaxial launcher makes the transition to 50 Ω microstrip without introducing appreciable discontinuities. The plane coil or impedance transformer is placed at the end of the microstrip circuit, which has provisions for placing capacitors in shunt and in series to tune out any inductive reactance of the coil or of the microstrip circuit itself.

LASER POWER FOR CONDUCTIVITY MODULATION

The measurement of excess carrier lifetime requires a pulsed increase in the conductivity of the semiconductor material using a pulsed laser with the photoconductivity decay transient monitored after termination of the laser light pulse. The power needed to produce a detectable conductivity change depends upon the dark conductivity of the semiconductor. A lower resistivity semiconductor requires a higher power laser to produce a detectable increase in conductivity. An approximate method for estimating the power of the laser is as follows.

The equation which governs the time behavior of the increase, ΔN, of the carrier concentration, N, is given by:

$$\frac{d}{dt}(AT\Delta N) = AN_{PH}(1-R) - \frac{AT\Delta N}{\tau} \tag{5}$$

where T is the thickness of the wafer, A is the area probed in the material, N_{PH} is the photon flux density, R is the reflectivity of the semiconductor wafer, and τ is the effective excess carrier lifetime taking into account bulk and surface recombination effects. For a laser pulse longer than τ, steady state solution is given by:

6

$$\Delta N = \frac{N_{PH}(1-R)\tau}{T} \tag{6}$$

The ratio of photon flux density to carrier concentration becomes:

$$\frac{N_{PH}}{N} = \frac{\Delta N}{N}\frac{T}{(1-R)\tau} \tag{7}$$

Assuming: .

$$\frac{\Delta N}{N} \approx 0.2, \ T \approx 0.05\,cm, \ R \approx 0, \ \tau \approx 10^{-7}s \tag{8}$$

the required N_{PH} is approximately 10^5 times larger than the carrier concentration N. Assuming that the carrier concentration is of the order of 10^{17} carriers/cm^3 and that the laser wavelength is approximately 1.3 μm (i.e. the photon energy is approximately 1 eV), the laser intensity is of the order of 1000 W/cm^2. Usually the area probed is of the order of 0.25 to 0.1 cm^2, so the laser power needed is of the order of 100 to 250 W. The new setup was designed for a Q-switched, 1.32 μm Nd:YAG laser with pulses of around 500 W .

RF MEASUREMENT SYSTEM DESCRIPTION AND CALIBRATION OF CAPABILITIES

The photoinduced RF reflectance decay system is a homodyne system implemented around a variable frequency RF oscillator (10~500 MHz) delivering up to +20 dBm (100 mW) into a 50 Ω load. A portion of this signal is fed to a probe card and any signal reflected back from the sample is mixed with the oscillator signal. Since the reflected signal has the same frequency as the oscillator signal, the mixer output will ideally contain two components -- one at twice the oscillator frequency and one at DC. By filtering out the high frequency components, the resultant signal will be proportional to the product of the magnitude of the reflected signal and the cosine of its phase relative to the oscillator output. This signal is then sampled on a digital scope for processing on a computer connected via the general-purpose interface bus (GPIB) interface. By using homodyne detection of the reflected signal, greater sensitivity is achieved over the diode detector of the microwave reflectance system.

A more detailed schematic of the RF system is depicted in Figure 5. The variable attenuator serves both to limit the power being fed to the probe card and to isolate the signal at the local oscillator (reference) port of the mixer from changes in loading. Following the attenuator is a 6 dB directional coupler which samples the signal reflected back from the probe card with a total of 12 dB loss. The reflected signal is then amplified by 25 dB and fed into the RF port of the mixer to be mixed with the 20 dB amplified signal from the oscillator. The latter amplifier is employed to provide a +23 dBm local oscillator signal necessary for good mixer performance, i.e., minimum insertion loss ~ 8 dB. The mixer output is then filtered by a diplexer consisting of a 50 MHz 5th order low-pass section in parallel with a 50 MHz 5th order high-pass section to shunt the higher frequencies into a matched load, as depicted in Figure 6.
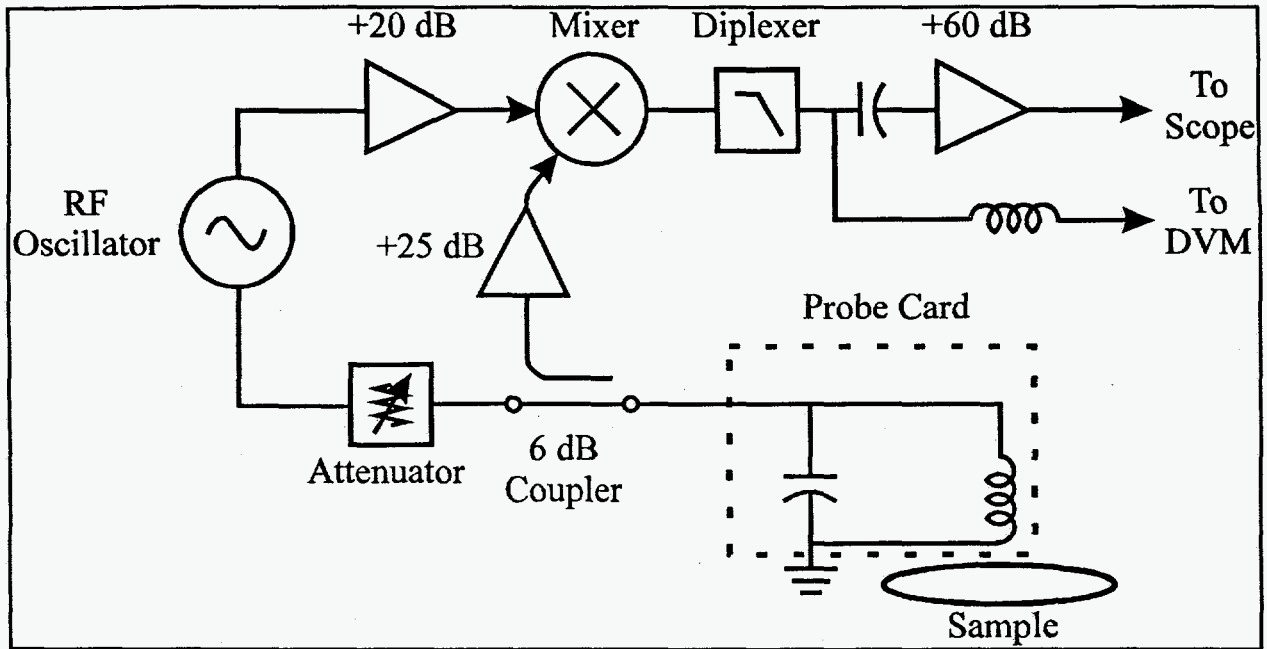
7

Figure 5. RF system layout
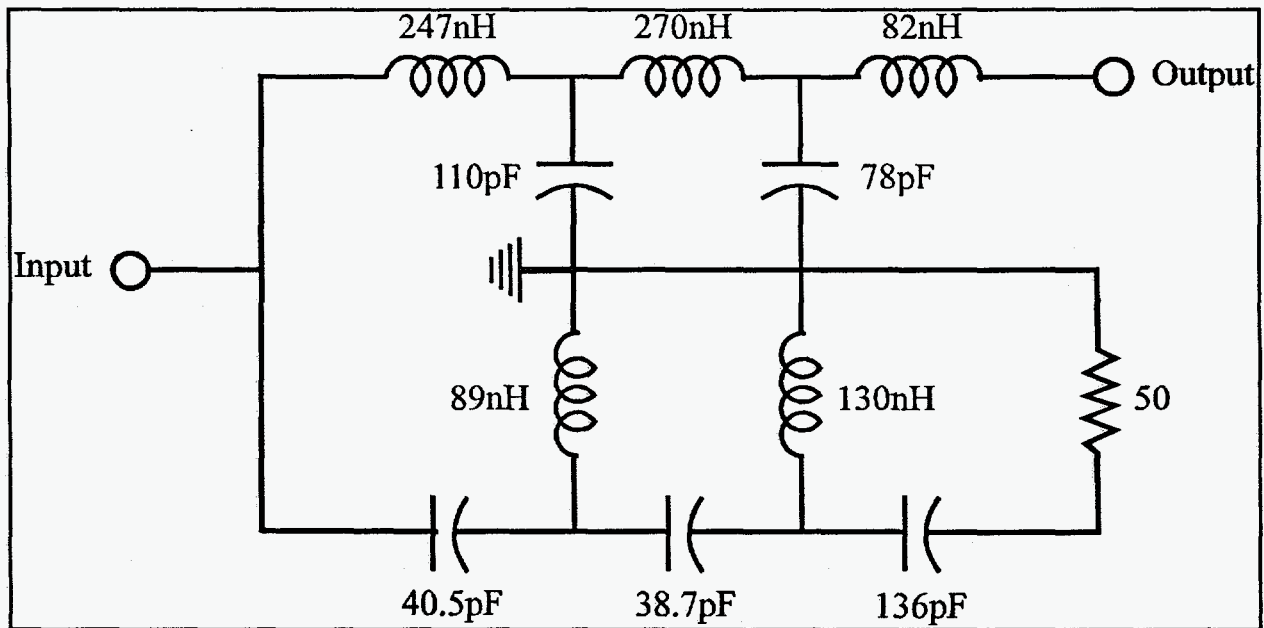
Figure 6. 50 MHz 5th-order Chebyshev diplexer

A low-pass filter alone would allow the rejected higher frequencies to be reflected back into the mixer which would distort the DC signal. The capacitor following the diplexer passes all but very low frequencies into a 60 dB amplifier to be sampled by the digital scope. The very low frequencies are passed by the RF choke into a digital DC voltmeter. The DC voltage is a measurement of the sheet resistance of the sample down to a depth on the order of the skin depth

8

of the RF signal in the material. The signal measured on the scope is sensitive to changes in the sample conductivity as brought about, for example, by photogenerated carriers excited during a laser pulse.

The probe card couples RF energy to the sample surface and detects the reflected signal with a minimum of loss. Since the rest of the system uses components with a 50 Ω characteristic impedance, the probe card utilizes 50 Ω microstrip transmission lines on a Duroid® (ε_r=2.2) microwave substrate. The probe card circuit is essentially a tuned RF transformer with the physical (variable) capacitor and coil in the primary, and the eddy currents induced in the sample as the secondary when the coil is in close proximity. The sheet resistance of the sample impeding the eddy currents is transformed into the primary circuit on the probe card. Therefore, the impedance is changed, which results in a change in the amount of signal reflected back to the mixer.

The probe card and transformer coils were initially characterized against materials of various conductivities on a network analyzer between 50 and 500 MHz to tune the variable capacitor and optimize the coil design for maximum sensitivity to the change in conductivity. With the circuit unloaded resonance set to 130 MHz using a 4 mm diameter one-turn coil, the probe card data from the network analyzer is shown in Figure 7 for 4 samples (2 Ω-cm Si, 0.03 Ω-cm Si, in-house grown GaSb boule, and a brass block (6.4 μΩ-cm)).

The left axes (Δ) show the magnitude of the reflected signals, in decibels (dB), and the
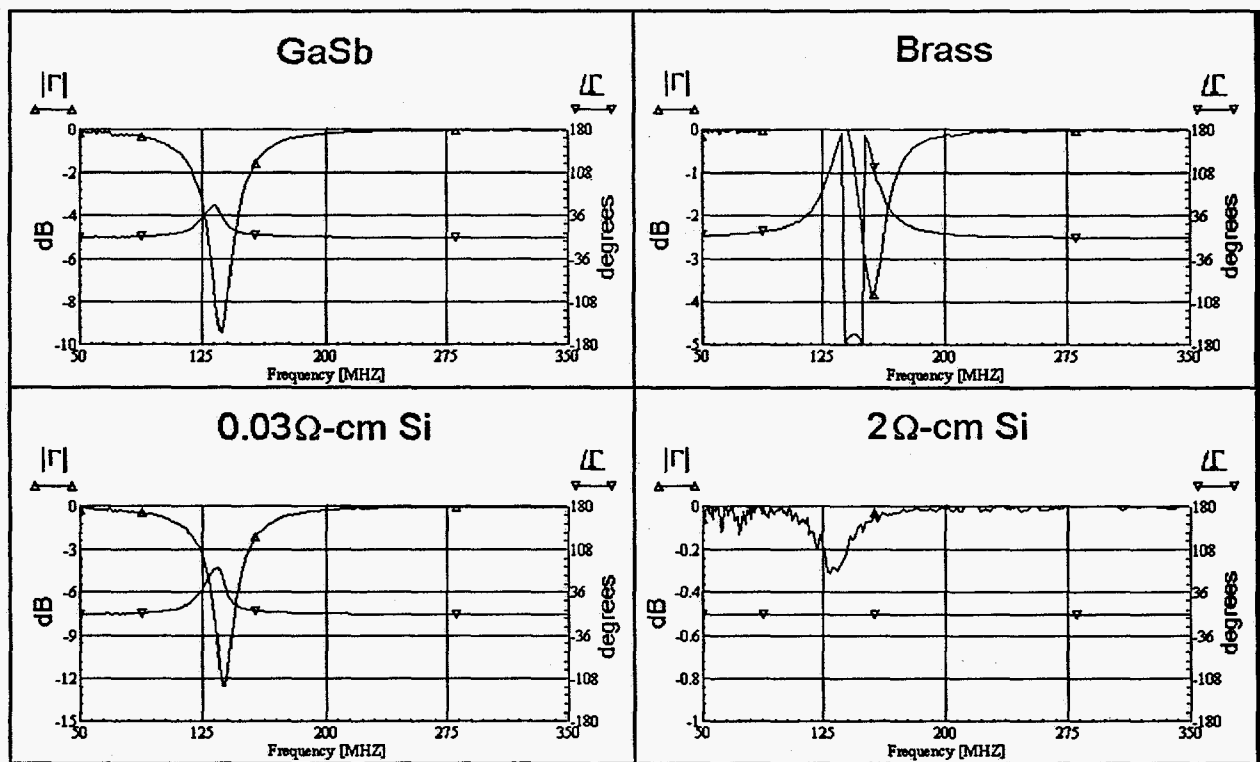

Figure 7. Network Analyzer Output with 4 mm 1-turn coil

9

right axes (∇) show the relative phase shift, in degrees, as functions of frequency (note: different scales are used on the left axes). From the amount of attenuation near resonance, i.e. minimum in |Γ|, this coil appears to have a useful range from 2 Ω-cm to 6.4 μΩ-cm, with a peak sensitivity between 0.03 Ω-cm and the resistivity of GaSb because of their approximation to a matched load. However, other factors, such as the minority carrier lifetime, diffusion length, optical absorption depth and the power of the optical pulses, decrease the actual useful range of the coil in the RF decay system. For the highly conducting brass sample, the phase shift near resonance is close to 180° so that the reflected signal is actually inverted.

The laser sources currently used in the RF decay system include a 10 ns, 80 W/pulse GaAs diode laser at 904 nm and a 1.5 μs, 800 W/pulse Q-switched Nd:YAG laser at 1.32 μm wavelength. The differences between these lasers have been characterized and are presented in Figures 8 and 9.
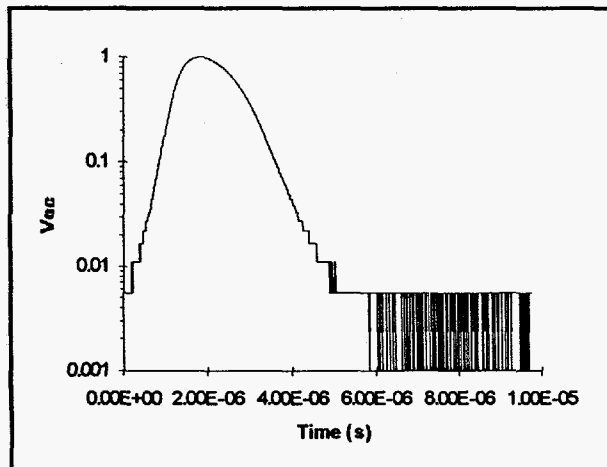

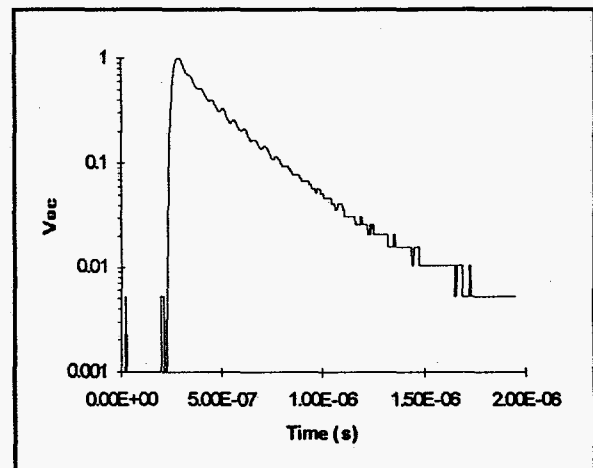**Figure 8a.** Open circuit response to YAG laser

Figure 8b. Open circuit response to GaAs laser

Figure 8 depicts the normalized open-circuit voltage (V_{OC}) measured with an InGaSb junction grown on a GaAs substrate with photoexcitation by YAG and GaAs lasers, respectively. The YAG response has a characteristic risetime of 0.26 μs and a decay time of 1.22 μs whereas the GaAs response risetime is 20 ns and the falltime is 0.25 μs. The true decay of the GaAs laser pulse is actually much faster than 0.25 μs, with this decay time being more representative of the actual recombination lifetime of the cell. However, since the V_{OC} decay from the YAG laser is much slower, the measured decay rate is an accurate profile of the optical decay of this laser.

Figure 9 shows the RF system response for the same high-resistivity GaSb substrate, demonstrating the effect of the optical pulse shape on the measured decay time. The response from the YAG laser has a characteristic risetime of 0.22 μs and a decay time of 0.78 μs, and the GaAs laser response has a risetime of 25 ns and a decay time of 0.26 μs. The fact that the measured RF risetime is 25 ns implies that the electronics of the RF system are capable of measuring such decay times. Thus, the GaAs laser provides a faster pulse which allows better
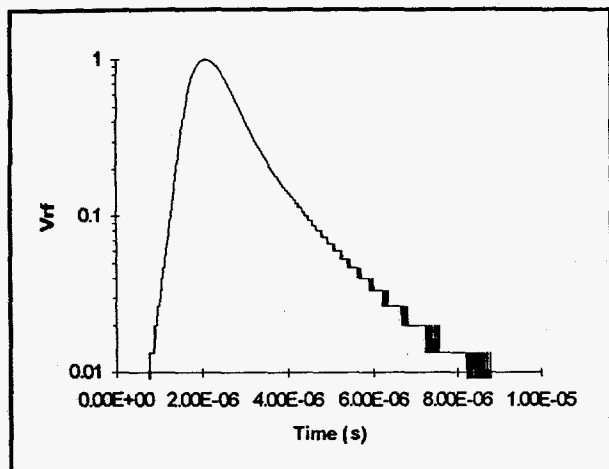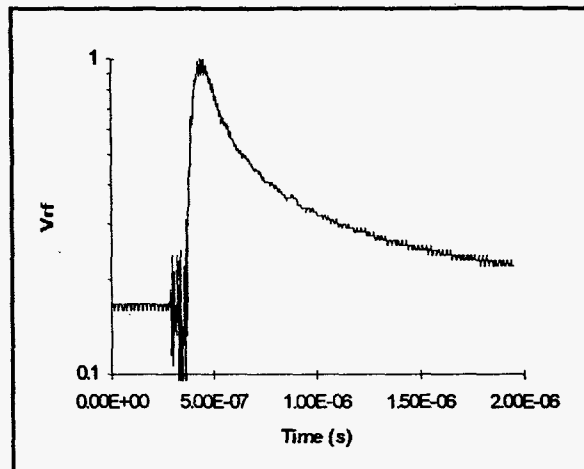
10

Figure 9a. RF Decay with YAG laser

Figure 9b. RF Decay with GaAs laser

resolution of the sample carrier lifetime, but has lower power and shorter wavelength which limits absorption depth to approximately 0.1 µm in GaSb. However, the YAG laser is capable of modulating the conductivity of relatively highly doped samples and has an absorption coefficient (α) of 1.4×10^4 cm^{-1} (corresponding to an effective absorption depth of 0.7 µm). In addition, a slow rise and fall time effectively places a lower limit on the measurement of decay to approximately 0.7 µs.

SEMICONDUCTOR MATERIAL MEASUREMENTS

Many GaSb samples have been measured using the RF non-contacting probe system: commercial substrates, in-house bulk substrates, Zn-diffused samples, and OMVPE layers. Typical data recorded includes the height of the reflected pulse (in mV), the risetime and decay time, the DC voltage as measured from the digital voltmeter, and the RF measurement frequency. The goal is to eventually be able to determine the quality and defect concentration in a given sample.

Commercial Substrates

Several substrates were measured from Firebird®, both p- and n-type, with doping concentrations from 5×10^{16} cm^{-3} to 8×10^{17} cm^{-3}. However, the samples doped higher than 10^{17} cm^{-3} did not yield measurable pulse signals (resolution presently 1 to 3 mV). The data for the 5×10^{16} cm^{-3} p-type substrates is summarized in Table 1.

The results indicate that the pulse height is very sensitive to the non-uniformities in the samples as the probe is moved from the edge of the sample to the center. The decay time increased by 19 % in FB1 and appears to double in FB202. However, the noise level of the system is around 1 mV making measurement of the decay time on small signals much less precise. In both samples, the use of the GaAs laser gives a pulse height ~30 % less than does the YAG laser (which can be attributed to differences in laser power), but much smaller decay times due to the difference in speed of the lasers. As mentioned above, the GaAs decay times are much

11

Sample	Pulse Height (mV)		Decay Time (μs)		DC Voltage (V)	Comments
	YAG	GaAs	YAG	GaAs		
FB1	1200	900	0.78	0.25	0.18	edge
FB1	32	<1	0.93	N/A	0.28	center
FB202	1350	832	2.73	0.44	0.25	edge
FB202	6	<1	5.31	N/A	0.28	center

Table 1. Measurement on p-type Commercial Substrates

closer to the sample carrier lifetime, but due to the much shorter absorption depth, is more sensitive to surface phenomena.

In-House Crystals

A quarter-inch thick, 32 mm diameter, undoped GaSb wafer from an in-house grown boule was mapped with the RF measurement system. This sample was of particular interest because of a twin boundary approximately 6 mm from the edge. Measurements depicted in Figure 10 were taken in 4 mm steps from the center along radii (A) toward the boundary, (B) away from the boundary, and (C) 45° from (B) towards the boundary.
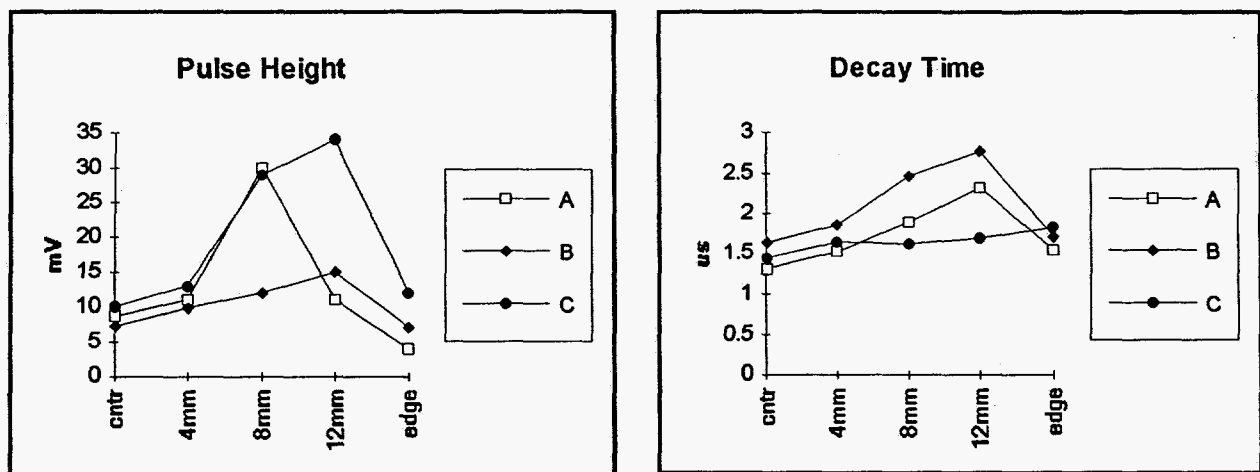

Figure 10. Pulse Height and Decay Time Spatial Distribution for Undoped GaSb Wafer

12

The DC voltage is azimuthally symmetric and does not vary significantly along the radials. Once again, the pulse height displays the greatest sensitivity to the presence of the defect (located at the 12 mm data point along path A). The pulse heights in scans B and C both increase monotonically until the rough and unpolished edge is reached; however, the pulse height in scan A decreases at the twin boundary. These results indicate a sensitivity to material quality, although an interpretation of the result is not clear.

Zn-Diffused Samples

Measurements were taken on commercial substrates from Firebird® (5×10^{16} cm^{-3} Te) and MCP® (10^{17} cm^{-3} Te) which underwent heavy ($\sim 10^{19}$ cm^{-3}) constant source Zn diffusions for various durations at 600°C. With the higher doped MCP® substrates, pulse data could not be obtained and the DC voltages were less than 0.070 V. The Firebird® data is shown in Table 2, ordered by the diffusion time.

Sample	Pulse Height (mV)		Decay Time (μs)		DC Voltage (V)	Diffusion Time
	YAG	GaAs	YAG	GaAs		
Unprocessed	1350	832	2.73	0.44	0.25	No diffusion
GP37	327	260	1.22	0.72	0.24	1 hr 20 min
GP33	46	40	0.90	0.46	0.28	4 hr
GP38	11	<1	0.95	N/A	0.28	5 hr 20 min
GP30	26	34	0.92	0.74	0.29	10 hr

Table 2. Measurements on Zn-diffused Samples (FB202 substrate)

The most prominent trend is the decreasing pulse heights (with either laser) as the sample is exposed to longer diffusion times. Since the DC voltage changes very little, the decrease in pulse height is attributed to the presence of higher concentrations of traps; this agrees with the presumption that the sample becomes more defected with deeper Zn diffusions. Also, a slight increase in the DC voltage is observed at deeper diffusions, indicating a higher sheet resistance. This trend suggests that the hole (majority carrier) mobility may be decreasing as well.

13

Epitaxial Samples

Measurements were taken on OMVPE samples consisting of p/n layers grown on an n-type graded layer on an n-type GaSb substrate, with and without metallization. The metallization is evaporated at low temperatures so that the grown layers are not significantly altered. The results are presented in Table 3 along with the thicknesses and dopings of the p/n layers.

The metallization was deposited in either large area metal windows and dots (#141, 142, and 146) for electrical characterization of the junction, or in a low density metal grid (#146) typical of TPV cells. In all three samples, the highly doped layers result in very low pulse heights, which increase over 30 times for both lasers with the addition of the metal. Also, the DC voltages decrease as a result of the decreased average sheet resistance due to the presence of the metal circles. The exception is the case of the low density metal grid where the pulse height increases by almost two orders of magnitude and the DC voltage increases. The presence of the grid concentrates the eddy currents into loops between the gridlines; therefore, the path length

Sample	Structure (all p on n with thicknesses and doping concentrations as indicated)	Pulse Height (mV)		Decay Time (μs)		DC Voltage (V)
		YAG	GaAs	YAG	GaAs	
141 (bare)	$3\mu m\ 8\times10^{17}$ /$1\mu m\ 5\times10^{17}$	3	<1	2.50	N/A	0.084
141 (metal circ)	same as above	90	20	2.77	2.13	-0.032
142 (bare)	$3\mu m\ 5\times10^{17}$ /$1\mu m\ 5\times10^{17}$	2.8	<1	2.51	N/A	0.137
142 (metal circ)	same as above	200	53	1.26	1.43	-0.019
146 (bare)	$0.3\mu m\ 5\times10^{17}$ /$4.5\mu m\ 7\times10^{17}$	3.3	<1	3.24	N/A	0.028
146 (metal circ)	same as above	110	48	2.21	1.74	0.009
146 (metal grid)	same as above	238	135	2.57	2.08	0.121

Table 3. Measurements on OMVPE samples (some decay times are not available (N/A) due to the low pulse response)

14

of the currents is increased, presenting a larger effective sheet resistance. As a result, the sensitivity is increased for the highly doped layers. In comparison, signals could not be detected with the 36 GHz microwave system for any of the GaSb samples evaluated.

SUMMARY AND CONCLUSIONS

A system which is capable of non-destructively discriminating defect concentrations in low bandgap materials has been demonstrated based on the pulse height and decay time of photogenerated carriers in the sample. With the current 4 mm diameter probe coil, the system can provide maps of defect levels across the surface of the sample with a 4 mm resolution. The system also has the capability of discerning the differences in the background doping of materials and can be used to map the variations of this quantity across the surface of a sample. Since it was designed around a characteristic impedance of 50 Ω, the RF system is better suited to make measurements on low-bandgap or heavier doped samples than is the microwave system. Evidence of this capability was found with the 2 Ω-cm Si, the 0.03 Ω-cm Si, and the FB1 GaSb substrate using the GaAs laser. The low-doped Si sample yielded a pulse on the RF system over twice as large as on the microwave system with decay times differing by only 3.5 %. A detectable pulse could not be obtained on either the heavily doped Si or the FB1 substrate with the microwave system.

The pulse height is the most sensitive parameter to variations in a given sample. High quality commercial substrates have almost two orders of magnitude variation in pulse height from center to edge. The mapping of the wafer containing a twin boundary, and the measurements on the Zn diffused samples are correlated to the presence of known defects.

The decay time shows less sensitivity to material quality, but has the advantage of being relatively unaffected by the background doping level as compared to the pulse height. The laser sources provide a measurement capability on samples with up to 10^{17} cm^{-3} n-type doping (limited only because of the low pulse heights). A decay time as low as 0.78 μs can be measured with the YAG laser and 20 ns with the GaAs laser. The latter corresponds to the theoretical limit of the system with a 50 MHz low-pass filter. However, decay times on this order cannot be measured with the GaAs laser presently due to the low pulse power. That is, the number of excess carriers generated is proportional to the carrier lifetime; in poorer material with a low lifetime a sufficient density of carriers for detection will not be generated. However, decay times as low as 0.25 μs have been demonstrated with the GaAs laser (see Table 1).

The system is sensitive to the positioning of the height of the probe card with respect to the sample. Also, since the laser power is fed to the sample via a fiberoptic cable, the finite divergence angle at the output of the cable means that the intensity of the laser illumination will vary with distance from the sample. Thus, the pulse height will be directly affected by the positioning of the fiber. Therefore, a mechanically stable probe card and fiber optic holder are required to achieve repeatable results.

References

1. J. M. Borrego, R. J. Gutmann, N. Jensen, "Non-Destructive Lifetime Measurement in Silicon Wafers by Microwave Reflection", *Solid-State Electronics* **30** No. 2, 195 (1987).

2. J. M. Borrego, R. J. Gutmann, N. Jensen, C. S. Lo, O. Paz, "Characterization of the DFZ in Silicon Wafers by a Non-Destructive Technique", *Mat. Res. Soc. Symp. Proc.* **69**, 373 (1986).

3. R. J. Gutmann, J. M. Borrego, C. S. Lo, M. C. Heimlich, O. Paz, "Microwave-Detected Photoconductivity-Transient Spectroscopy for Non-Destructive Evaluation of GaAs Wafers", *SPIE* **794**, 128 (1987)

4. M.C. Heimlich, R. J. Gutmann, D. Seielstad, D. Hou, "Damage-Induced Effects in Co-Implanted LEC GaAs", *6th Conf. on Semi-ins. III-V Mat.*, 367 (1990)

5. R. J. Gutmann, M. C. Heimlich, M. Tait, T. B. Bylsma, E. Monberg, "Photoinduced Microwave Reflectometry as a Non-Invasive Technique for S. I. InP Wafer Characterization", *6th Conf. on Semi-ins III-V Mat.*, 323 (1990)

6. M. C. Heimlich, E. R. Atwood, R. J. Gutmann, "Two-Dimensional Mapping of Implantation and Annealing Phenomena in GaAs by Photoinduced Microwave Reflectometry", *Semicond. Sci. Tech.* **7**, A275 (1992)

7. M. C. Heimlich, R. J. Gutmann, L. Kerber, S. Moreau, J. Vaughan, "Characterization of Active Channel Processing by PIMR", *7th Conf. on Semi-ins Mat.*, 291 (1992)

8. E. Yablonovitch, T. J. Gmitter, "A Contactless Minority Lifetime Probe of Hetero-structures, Surfaces, Interfaces, and Bulk Wafers", *Solid-State Electronics* **35** No. 3, 261 (1992).